Computers in Biology and Medicine 148 (2022) 105791

Contents lists available at ScienceDirect

Computers in Biology and Medicine

journal homepage: www.elsevier.com/locate/compbiomed

Investigating the discrimination of linear and nonlinear effective connectivity patterns of EEG signals in children with Attention-Deficit/Hyperactivity Disorder and Typically Developing children

Nasibeh Talebi, Ali Motie Nasrabadi *

Department of Biomedical Engineering, Faculty of Engineering, Shahed University, Tehran, Iran

ARTICLE INFO

Keywords:
Attention deficit hyperactivity disorder (ADHD)
Linear and nonlinear effective connectivity
EEG
Direct directed transfer function
ADHD detection

ABSTRACT

Background: Analysis of effective connectivity among brain regions is an important key to decipher the mechanisms underlying neural disorders such as Attention Deficit Hyperactivity Disorder (ADHD). We previously introduced a new method, called nCREANN (nonlinear Causal Relationship Estimation by Artificial Neural Network), for estimating linear and nonlinear components of effective connectivity, and provided novel findings about effective connectivity of EEG signals of children with autism. Using the nCREANN method in the present study, we assessed effective connectivity patterns of ADHD children based on their EEG signals recorded during a visual attention task, and compared them with the aged-matched Typically Developing (TD) subjects.

Method: In addition to the nCREANN method for estimating linear and nonlinear aspects of effective connectivity, the direct Directed Transfer Function (dDTF) was utilized to extract the spectral information of connectivity patterns.

Results: The dDTF results did not suggest a specific frequency band for distinguishing between the two groups, and different patterns of effective connectivity were observed in all bands. Both nCREANN and dDTF methods showed decreased connectivity between temporal/frontal and temporal/occipital regions, and increased connection between frontal/parietal regions in ADHDs than TDs. Furthermore, the nCREANN results showed more left-lateralized connections in ADHDs compared to the symmetric bilateral inter-hemispheric interactions in TDs. In addition, by fusion of linear and nonlinear connectivity measures of nCREANN method, we achieved an accuracy of 99% in classification of the two groups.

Conclusion: These findings emphasize the capability of nCREANN method to investigate the brain functioning of neural disorders and its strength in preciously distinguish between healthy and disordered subjects.

1. Introduction

Attention deficit hyperactivity disorder (ADHD) is one of the most common neurodevelopmental disorders in children characterized by inattention, or excessive activity and impulsivity which may cause behavioral, psychological, academic, and social difficulties throughout the lifespan [1]. Accurate and rapid diagnosis of ADHD would be beneficial to clinical studies exploring more effective treatments of this disorder. Over the years, researchers have used various neuroimaging modalities and analysis methods to gain deeper information about ADHD. Estimation of brain connectivity measures from Electroencephalography (EEG) signals have especially received a lot of attention. EEG is a clinically available and relatively inexpensive neuroimaging technique that allows for the capturing of a wide range of brain processes [2], and brain connectivity techniques treat the pathophysiology of neuropsychiatric disorders from a system perspective. Characterizing the atypical patterns of whole-brain system would be helpful for better understanding the neurodevelopmental disorders, since a coherent interaction between the brain regions has a critical role in the human's cognition and behavior [3,4].

The two main methods for analyzing connectivity between brain regions are functional connectivity and effective connectivity. Functional connectivity refers to the statistical dependencies between brain activities in different regions, and effective connectivity is the influence that one region exerts over another.

The extensive EEG studies on ADHD have found abnormalities not

* Corresponding author.
E-mail addresses: nasibeh.talebi@gmail.com (N. Talebi), nasrabadi@shahed.ac.ir (A. Motie Nasrabadi).

https://doi.org/10.1016/j.compbiomed.2022.105791
Received 26 April 2022; Received in revised form 6 June 2022; Accepted 26 June 2022
Available online 10 July 2022

only in the activity of various brain regions in the individuals with ADHD, but also in the interdependencies between these regions [5,6]. Most of the previous EEG based connectivity studies have evaluated functional connectivity in ADHD subjects. There are some hypo [7–9]- or hyper [7,9,10]-connectivity depending on the frequency band, mental task and functional connectivity measure computed from intra-hemispheric or inter-hemispheric EEG channel pairs [11].

Although functional connectivity describes the synchronization between the regions, it does not necessarily reveals the direction of influence of some neural systems over others. To provide additional information about the direction of interactions as well as their presence, the effective connectivity notion is developed [12]. In the field of ADHD research, some studies have used EEG data to assess the effective connectivity patterns of ADHD subjects and make a classification based on these measures.

In a study by Muthuraman et al., they used partial directed coherence (PDC) to measure the effective connectivity of resting state EEG signals at different frequency bands. The authors reported unidirectional connectivity profile in patients with ADHD rather than bidirectional interregional connectivity exhibited in TDs [44]. Furthermore, they utilized support vector machine (SVM) to classify ADHD/TD groups and achieved an accuracy of 98% by combining features from all five studied frequency bands. In another EEG based study, Ekhlasi et al., applied directed phase transfer entropy method to investigate the differences of effective connectivity in ADHD and TD children while they were performing a visual attention task [15]. They observed differences between two groups in theta, beta, and delta bands. In beta band, the connectivity was greater for TDs while in delta frequency bands it was greater for ADHDs. They also classified these two groups based on the connectivity measures and achieved the best result (89.7%) for theta frequency band [14]. Using the same dataset, Abbas et al., applied transfer entropy technique to evaluate pair-wise directed information flow between EEG signals within various frequency bands, and found that the measures in beta band has the greatest discrimination between the ADHD and TDs [16].

Although the above mentioned methods have proved advantages in assessment of ADHD, there are still some measures of brain connectivity, which have not been investigated for this disorder. Furthermore, the PDC measure used by Muthuraman et al. [44] is computed based on the coefficients of the linear multivariate autoregressive (MVAR) model. However, regarding the widespread assumption about the nonlinear interactions among neuronal populations [45–47], using just the linear connectivity measures may be not adequate for comprehensive causal analyses among brain regions. The Transfer Entropy technique used by Ekhlasi [15] and Abbas [16] is a nonlinear method that contains the information of both linear and nonlinear interaction based on information theory. This method, however, does not explicitly distinguish between linear and nonlinear connectivity.

In our previous work, we developed a new causal relationship estimator, called nCREANN (nonlinear Causal Relationship Estimation by Artificial Neural Network), that estimates both linear and nonlinear effective connectivity and has a unique ability to distinguish between these two types of interactions [13]. This method has the potential to bring new insights about ADHD.

In the present study, we assess the linear and nonlinear aspects of effective connectivity patterns in ADHD subjects by applying the nCREANN on the current sources reconstructed from EEG recordings. We also use dDTF (direct Directed Transfer Function) method to extract the spectral information of connectivity patterns in ADHDs and TDs. Furthermore, we evaluate the capability of these measures in classification of ADHD/TD subjects.

The estimated connectivity values are statistically analyzed for significant differences. Afterward, we use well-known machine learning methods including (Linear Discriminant Analysis (LDA), K-Nearest Neighbor (KNN), Support Vector Machine (SVM), and MLP-ANN) to classify the ADHD and TD groups and to discover biomarkers for discriminating these two groups. The dataset used in this study is the same as the work of [14–16], which has been recently released in IEEE dataport [17].

2. Material and methods

2.1. EEG dataset

Participants were 61 children with ADHD and 60 healthy Typically Developing (TD) subjects (boys and girls, ages 7–12) [17]. The ADHD children were diagnosed by an experienced psychiatrist to DSM-IV criteria [18]. None of the children in the TD group had a history of psychiatric disorders, epilepsy, drug abuse, head injury, or any report of high-risk behaviors.

EEG recording was performed based on 10–20 standard by 19 channels (Fz, Cz, Pz, C3, T3, C4, T4, Fp1, Fp2, F3, F4, F7, F8, P3, P4, T5, T6, O1, O2) at 128 Hz sampling frequency. The A1 and A2 electrodes were the references located on earlobes. The eye movement was recorded by two electrodes that were placed below and above the right eye.

Since ADHD children have deficits in attention, the EEG recording protocol was based on a visual attention tasks. In the task, a set of pictures of cartoon characters was shown to the children and they were asked to count the characters. The number of characters in each image was randomly selected between 5 and 16, and the size of the pictures was large enough to be easily visible and countable by children [19]. This dataset is available at *https://ieee-dataport.org/open-access/eeg-data-adhd-control-children*.

2.2. EEG data preprocessing

All preprocessing was carried out by EEGLAB toolbox and through MATLAB software [20]. The EEG recordings were first visually inspected for identification of large artifacts (such as excessive muscular artifacts, high electrode impedance, or amplifier blocking) [21], and noisy segments were manually rejected. The ‘cleanline’ plugin was used for attenuating the line noise, and the data was passed through a 0.5Hz high-pass filter before implementing the independent component analysis (ICA). The ocular, muscular, cardiac, and other artifacts were removed using ICA. The characteristics of the time series and the power spectrum of the clean EEG signals were assessed based on the criteria explained in the literature [22,23].

Estimation of effective connectivity directly from EEG signals may be affected by the volume conduction effect, which may cause serious confounding results [24]. A common solution is to first reconstruct the underlying sources via an inverse method on EEG recordings, and then to measure the connectivity for the extracted sources. Here, for the source reconstruction procedure we applied multiple sparse priors (MSP) algorithm through the Statistical Parametric Mapping (SPM) software package [25]. The SPM toolbox is available online at http://www.fil.ion.ucl.ac.uk/spm/.

The SPM’s template head model was utilized for source localization. The voxels with the maximal activity were identified. Then, throughout of 100 nearest voxels to the maximum voxel, 10 voxels with the next greatest activities were selected and the average of their time courses was considered as the signal of the brain source of that region. This procedure was performed for both ADHD and TD groups and 8 regions with the highest activity were selected. For each group, the source reconstruction process was performed separately, but all individuals within a group were considered simultaneously for the resource reconstruction process (using the group inversion option in SPM). The MNI (Montreal Neurological Institute and Hospital) coordinates of the regions of interest (ROIs) for both groups are given in Table 1.

Table 1
MNI Coordinates of sources with maximal activity in the ADHD and TD groups.

ADHD				TD			
x	y	z		x	y	z	
−44	38	14	frontal	−26	58	8	frontal
46	46	10		16	56	0	
−52	−48	24	temporal	−52	−38	24	temporal
50	−48	22		54	−38	22	
−14	−54	68	parietal	−50	−42	56	parietal
18	−54	68		24	−40	54	
−12	−98	−8	occipital	−8	−94	−6	occipital
12	−92	−8		24	−98	−6	

2.3. Effective connectivity analysis

2.3.1. dDTF

The direct Directed Transfer Function (dDTF) is the modified version of DTF that represents only the direct causal link between the regions [26]. This measure is the frequency domain description of the directed linear relationship between time series. Using the SIFT plugin [27] of the EEGALB toolbox, in this study, the values of dDTF were calculated from the source signals at the following frequency bands: delta (0.5–4 Hz), theta (4–7 Hz), alpha (8–14 Hz), beta (15–30 Hz), and gamma (>30 Hz). For every subject, a MVAR model was first fitted to the signals of 8 brain regions. After fitting the model, it was validated using the default SIFT criteria (i.e. the whiteness of the model residuals, consistency of the model, and the stability/stationarity of the model). All the connectivity measures (dDTF and nCREANN) were estimated using the total length of the signals (about 2 min) and without windowing. For all subjects, the optimum model order was evaluated using Akaike and Schwartz criteria [28]. This model order ($p = 10$) was considered the same for all subjects.

2.3.2. nCREANN

For the nCREANN method, a nonlinear MVAR model (eq. (1)) is fit on the current source signals:

$$\mathbf{x}(\mathrm{n}) = \mathbf{f}(\mathbf{x}_\mathrm{p}) + \boldsymbol{\sigma}(\mathrm{n}) \tag{1}$$

Where

$$\mathbf{x}_p = [x_1(n-1), x_2(n-1), \cdots, x_M(n-p)]^\mathrm{T} \tag{2}$$

is the vector of p previous samples of (M) multivariate time series, and $\boldsymbol{\sigma}(n) = [\sigma_1, \sigma_2, \ldots, \sigma_M]^T$ is the model residual. This model is implemented by a single-hidden-layer feed-forward network. During the training, subsequent samples, o_l, as the network's outputs, are predicted based on previous samples of all regions ($\mathbf{x}_p$).

Equation (3) describes the nonlinear MVAR model implemented by the network with N_i inputs, one hidden layer with N_h (nonlinear) neurons, and N_o (linear) output neurons.

$$o_l = \sum_{k=1}^{N_h} v_{kl}\left(a_k \tanh\left(b_k\left(\sum_{q=1}^{N_i} w_{qk}x_q\right)\right)\right) \tag{3}$$

Where w_{qk} is the connecting weight between kth hidden neuron to the qth input node, x_q, and a_k, b_k are the scaling parameters of $\tanh(.)$, and v_{kl} is the connecting weight of the lth output neuron and the kth unit in the hidden layer.

This produces a nonlinear MVAR model that expresses how the p previous samples cause the present values ((1)) [29], and the information about its coefficients is embedded in the network's parameters [30].

To extract the linear and nonlinear connectivity pattern between the input and output of the network, the Taylor expansion of the hidden neurons' activation function was used to segregate the linear and nonlinear parts of $\mathbf{f}(.)$. The linear part represents the linear interactions among the regions (input signals), while the nonlinear part contains the information about their nonlinear relationship.

2.3.2.1. Linear Causality coefficients. Based on the linear part of $\mathbf{f}(.)$, the *Linear Causality coefficient* (lCc_{lq}) represents the linear influence of qth input node on the lth output neuron.

$$Cc_{lq} = \sum_{k=1}^{N_h} a_k b_k w_{qk}.v_{kl}\ , \quad q = 1:N_i\ ,\ \ l = 1:N_o \tag{4}$$

Since in this study, the network input nodes are delayed samples of time series, and the outputs are subsequent samples of all signals, the *lCc* measures explain the relationship between the past and future of the signals and represent temporal causality (effective connectivity) between regions.

2.3.2.2. Nonlinear effective connectivity. The nonlinear directed interactions may be considered from two points of view: 1) *Nonlinearity* and *Nonlinear Information Inflow* which explain how much each region is influenced by the nonlinear interactions of itself and the others; and 2) *Nonlinear Effect* which represents the nonlinear effect of one region onto the others.

- *Nonlinearity* and *Nonlinear Information Inflow:*

For each ROI, the *Nonlinearity* is defined based on the difference between the linear and nonlinear portions of the output neurons corresponding to that region

$$Nonlinearity_l = 1 \Big/ \mathrm{L}\left(\sum_{\mathrm{n}=1}^{\mathrm{L}} \left|o_l - o_l^{Lin}\right|\right) \tag{5}$$

Where o_l^{Lin} is a part of the lth output generated only by the linear interactions of the inputs, and L is the length of the signal. If an output neuron contains nonlinear information from other signals, its *Nonlinearity* will have a non-zero value.

The second measure for identifying the nonlinear effects of inputs on an output is called *Nonlinear Information Inflow* (*NII*) and is defined as the ratio of the estimation errors where the predictions are made through only linear interactions of the inputs, ε_l^{lin}, to the case in which both linear and nonlinear interactions among input signals are considered, ε_l. The non-zero value of NII_l can be inferred as the existence of the nonlinear causal effects of the inputs on the lth output.

$$NII_l = \ln\left(\frac{\left(\varepsilon_l^{lin}\right)^2}{\left(\varepsilon_l\right)^2}\right) \tag{6}$$

- Nonlinear Effect

Although the above nonlinear measures reveal how a region is nonlinearly influenced by other regions, they do not indicate which region (input signal) has the nonlinear causal effect on the target region (output). To address this issue, the third nonlinear measure, *Nonlinear Effect* (*NE*) of x_α to x_l is defined again by the ratio of the estimation errors, but in this case, at the numerator, only the nonlinear effects of x_α are removed, and other ROIs have both linear and nonlinear influence on x_l. The denominator is the same as the NII_l. The $NE_{\alpha\to l}$ determines how much x_α has direct nonlinear causal effect on x_l.

$$NE_{\alpha\to l} = \ln\left(\frac{\left(\varepsilon_l\right)_{x_\alpha - Lin}^{\ 2}}{\left(\varepsilon_l\right)^2}\right) \tag{7}$$

Where $(\varepsilon_l)_{x_\alpha - Lin}$ is the prediction error of x_l, by including the linear effect of x_α, and ε_l is the prediction error by considering both linear and nonlinear effects of x_α.

2.4. Statistical analysis

Before performing the statistical test to find the significant differences between the two groups, the normality of connectivity values were checked using Jarque–Bera test [31]. All the coefficients did not have a normal distribution. Therefore the non-parametric Wilcoxon signed rank test [32] was used as an alternative to the paired Student's t-test.

2.5. Classification

After finding the connectivity values with significant differences between the ADHD and TD groups, they were classified using LDA, KNN, SVM, and ANN classifiers. The classification was performed for the following cases: 1) dDTF values averaged in each frequency band, and the combination of the features in all frequency bands; 2) absolute values of *lCc* (averaged for all time lags); 3) nonlinear connectivity measures (*Nonlinearity*, *NII*, and *NE*); 4) fusion of linear and nonlinear connectivity values of nCREANN.

The classification accuracy of the classifiers is defined as follows (TP: True Positive; TN: True Negative; FP: False Positive; FN: False Negative):

$$Accuracy = 100 * \frac{(TP + TN)}{(TP + TN + FP + FN)} \quad (8)$$

The classification procedure was evaluated using the k-fold (k = 10) cross-validation approach. 90% of data was considered as the training set and 10% was devoted to the test. The principal component analysis (PCA) technique was used for feature selection (the number of selected features for each feature set was between 11 and 16). For the ANN classifier, a feedforward network with one hidden layer and 7 hidden neurons was trained with the Levenberg-Marquardt backpropagation algorithm. The SVM classifier utilized radial basis function (RBF) kernels, and the number of neighbors in the KNN classifier was set to 5. The remaining parameters of ANN, SVM, and KNN, and all parameters of the LDA classifier were kept the same as the default values in MATLAB.

3. Results

3.1. dDTF

The computed dDTF coefficients for each subject were 64× 8 × 8 matrices, where 8 is the number of brain regions and 64 is the half sampling frequency. For each matrix, the average values in different frequency bands (delta, theta, alpha, beta, and gamma) were calculated.

The dDTF values averaged on all subjects in each group, are represented in Fig. 1 by connectivity arrows pointing from one region toward another, where the thickness of the arrows shows the connectivity strength. To avoid cluttering the images the most prominent connections were drawn. To find a threshold for displaying the effective connectivity vectors between the two regions, the average of the connectivity values in each frequency band was computed for each ADHD/TD group, and the minimum of these two mean values was considered as the threshold for that band. These threshold values for delta to gamma bands were 0.0452, 0.0354, 0.0246, 0.0127 and 0.0062, respectively.

As can be seen in this figure, there are strong connections (above the threshold) in all frequency bands from the temporal to frontal, and occipital lobes in TDs, while such connectivity is not observable in ADHD groups. Furthermore, in all frequency bands a bi-directional connectivity is seen between temporal and left frontal lobes which is not seen in TDs. Additionally, interhemispheric bidirectional connectivity between temporal, parietal and occipital lobes is only observable in ADHD group. And finally, while connectivity from temporal to parietal regions is observed in all frequency bands in TDs, in ADHDs such connection is only seen in beta and gamma bands.

3.2. nCREANN: Linear Causality coefficients

The mean absolute values of all non-self *linear Causality coefficients* averaged for all time lag and all subjects are shown in Fig. 2. Similar to Fig. 1, here we only showed stronger connections (It should be noted that different colors in Figs. 1, Fig 2, and Fig 4 is just for representing different types of connectivity measures and the colors do not show the magnitude of the connections). These measures show more connectivity among all regions in TD groups than ADHDs. Although there are significant linear connectivity among frontal, temporal, and parietal regions in ADHDs, there is not a considerable connection from their temporal and occipital lobes to other regions. In addition, a tendency to the left laterality is observed in the frontal connectivity pattern of ADHD groups, while in TDs there is symmetric interhemispheric information flow among the regions.

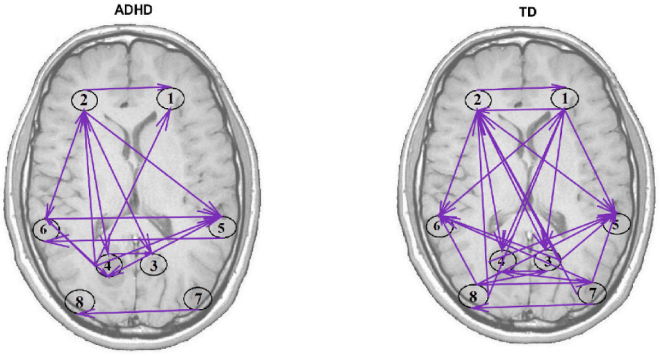

Fig. 2. Mean absolute values of *linear Causality coefficients* calculated by nCREANN method in two groups of ADHD (left) and TD (right). There is left lateralized connectivity with frontal region in ADHD group and the symmetric interhemispheric information flow among the regions in TD group.

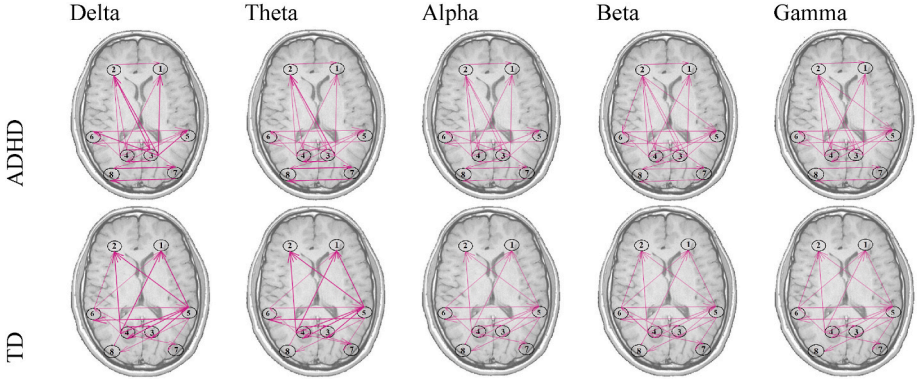

Fig. 1. Mean values of dDTF over all subjects in each ADHD (high) and TD (low) group which is shown in five frequency bands. Connectivity arrows point from one region toward another. In order to avoid crowding the images, only strong connection were shown. There are some differences between connectivity patterns of TD and ADHD groups. In TDs, a strong connectivity is seen between temporal/frontal, and temporal/occipital regions. In ADHDs, dominant bidirectional connection is observed between parietal/frontal regions.

3.3. nCREANN: Nonlinear connectivity

The results of Fig. 3 are the mean and standard error in the two parameters *Nonlinearity* and *Nonlinear Information Inflow* (*NII*). These values indicate the amount of only nonlinear influences on each region. As shown in the figure, for most regions, these nonlinear parameters are larger for the TD group than ADHDs.

Furthermore, Fig. 4 shows the *Nonlinear Effect* (*NE*) values for the two groups. Here, the values for all individuals in each group were averaged on all the subjects in each group, and each vector represents the nonlinear effect of one region on another. It can be seen that the nonlinear effective connectivity in the TD group is larger than the ADHD group for all regions. There is not significant directed nonlinear connection from temporal to frontal and occipital regions and from occipital lobes to the others. Furthermore, the nonlinear effective connectivity pattern in ADHDs is left lateralized, but the TD group has bilateral interhemispheric nonlinear interactions.

3.4. Classification

The ADHD/TD classification accuracy is shown in Table 2. The best results for dDTF coefficients was 98.18% for the fusion of the features from all frequency bands. Each frequency bands resulted in rather high accuracy (>96%). For the nCREANN method, the linear connectivity (*lCc*) achieved its best accuracy with 96.44%, while for nonlinear connectivity coefficients (*Nonlinearity*, *NII*, and *NE*) it was 86.82%. The fusion of linear and nonlinear connectivity values of nCREANN yielded in the best classification result (99.09%) with maximal average (mean) accuracy and the minimal standard deviation (SD).

4. Discussion

In this study, we estimated linear and nonlinear effective connectivity in children with ADHD and compared them with TD subjects. The connectivity measures were computed from the current sources reconstructed from EEG recordings of a visual attention task. The well-known linear method, dDTF, was applied for investigating the frequency content of connectivity patterns in two groups. Furthermore, our previously developed nonlinear method, nCREANN, estimated both linear and nonlinear components of effective connectivity and showed variation between ADHD/TD groups. We furthermore, explore these measures for the quantification of the best connectivity-based biomarker in ADHD. The measures with statistically significant differences were utilized to classify ADHD/TD groups by several classifiers.

The main finding of this study can be expressed from four perspectives: 1) In the frequency domain, there were differences in dDTF connectivity patterns between ADHDs and TDs in all bands, and the dDTF results did not specify any specific frequency band as a biomarker; 2) Regionally, there were differences in connectivity between the temporal/frontal, temporal/occipital, and parietal/frontal regions in two groups 3) The linear/nonlinear effective connectivity results by nCREANN showed more dominant linear and nonlinear interactions in

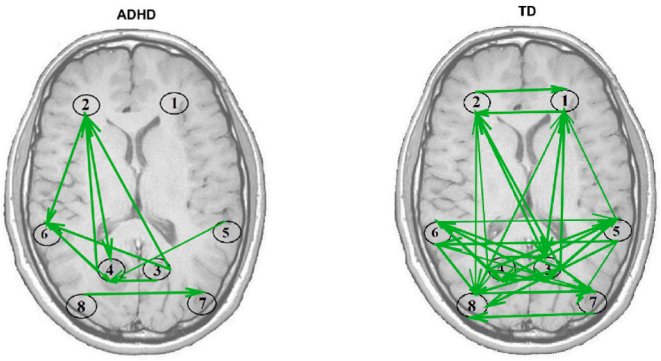

Fig. 4. *NE* values that are averaged for all individuals in each ADHD (left) andTD (right) groups. Nonlinear connections in the TD group are more and larger than in ADHD.

TDs than ADHDs, and in ADHDs the connections were left-lateralized compared with (almost) symmetric interactions in TDs; 4) And finally, from the classification point of view, based on connectivity values as the classifying features, we achieved the great accuracy of 99% in distinguishing between ADHD and TD subjects.

The dDTF values in all frequency bands in Fig. 1, and the pure linear and nonlinear connectivity maps in Fig 2, and Fig 4 showed some similarities and differences between the two groups. In both groups, there were strong connections between the frontal and the parietal regions. This similarity is in line with previous attentional task studies of ADHD and healthy groups [33]. According to the literature, both frontal and parietal lobes are core regions for attention processing and cognitive control tasks in the human brain [34]. However, there were more bidirectional relationships between the frontal and parietal regions in ADHD than TDs. The enhanced frontal-parietal connectivity in ADHD subjects may serve as an alternative, compensating their deficit in the early information integration stage to facilitate their accomplishing the attentional task [7].

The dDTF result in all frequency bands also showed attenuated connectivity from temporal to frontal, and occipital lobes in ADHDs, rather than TD group. This different pattern was also observed in nCREANN results (Figs. 2 and 4), which is in accordance to the previous findings of other studies [7,15,16,35]. Due to the absence of a dominant temporal/frontal/occipital network hub in ADHDs, their cortical network is assumed such a vulnerable that cannot tolerate the transient attenuations in activation of the attention network hubs in sustained attention tasks, which is consequently yielded to poorer performance in ADHD subjects [35].

Furthermore, the nCREANN results revealed that the ADHD maps tend to be more left-lateralized than TD subjects with almost symmetric interhemispheric connectivity patterns. This abnormality in the right hemisphere was also found in previous fMRI studies where ADHDs showed a hyper-functioning in the left frontal regions [35], and reduced activation in right inferior and orbital frontal and in bilateral

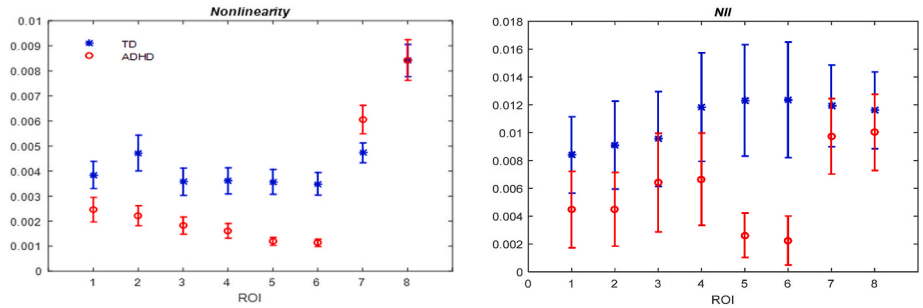

Fig. 3. *Nonlinearity* and *NII* parameters for 8 regions in two groups of TD (blue *) and ADHD (red ○).

Table 2
The classification accuracy(%) of various connectivity measures by different classifier.

Method		ANN		SVM		KNN		LDA	
		Mean	SD*	Mean	SD	Mean	SD	Mean	SD
dDTF	delta	94.85	5.93	97.42	4.15	96.44	6.29	92.95	5.68
	theta	94.70	6.27	96.44	6.29	97.42	4.15	89.32	11.09
	Alpha	89.62	10.61	97.27	4.39	96.44	6.29	87.65	10.86
	Beta	91.89	11.69	96.59	4.41	93.11	8.66	90.23	7.81
	gamma	93.71	6.10	96.44	6.29	95.61	6.02	92.95	6.91
	All dDTF frequency band	96.36	4.69	97.35	4.27	**98.18**	3.83	93.71	6.10
nCREANN	*lCc*	96.44	6.29	97.35	4.27	97.42	4.15	90.45	8.43
	Nonlinear connectivity	86.82	9.46	83.18	9.53	84.02	8.38	84.17	10.63
	All nCREANN measures	**99.09**	2.87	93.79	7.43	98.26	3.68	98.26	3.68

*SD: Standard Deviation.

temporo-frontal cortices as well as reduced functional networks connecting the occipital lobes with other cortical regions [5,36]. This pattern was also found in EEG studies [14,37,38]. Compared with TD subjects, Makris et al., found significant cortical thinning in ADHD in a distinct cortical network supporting attention especially in the right hemisphere [39]. Furthermore, Geurts et al., showed that ADHD is related to the deficits in grey-matter volume with the right parietal lobe, right temporal frontal cortex, bilateral thalamus, and left hippocampus/amygdala complex [40].

Although to up to our knowledge, the nCREANN is the only connectivity estimator that purely estimates linear and nonlinear effective connectivity, there are several studies applied nonlinear methods to investigate ADHDs brain functioning from connectivity, complexity or nonlinear dynamics point of view. Using approximate entropy (ApEn) as a non-linear information-theoretic measure, Sohn et al., reported significantly lower mean ApEn of the ADHD subjects than the healthy subjects over the right frontal regions during the performance of an auditory cognitive task, but this was not observed at resting state EEG recordings [41]. Fernández et al., reported reduced Lempel-Ziv complexity in resting state MEG signals of ADHD subjects than TDs [42]. Looking at the nCREANN results in Figs. 2, Fig 3, and Fig 4, one can inference that generally, there are more connections (both in terms of linear and nonlinear interaction) in TD subjects than in ADHDs during performing a visual attention task. In our previous work, we applied nCREANN method to resting-state EEG dataset of children with Autism Spectrum Disorder (ASD), and found more linear connectivity in TDs, but more nonlinear interactions in ASDs [13]. Assessment of the different patterns of nonlinear interactions in ASD and ADHD subjects could be considered as our future works.

After estimating various effective connectivity measures, we utilized those with statistically significant differences between ADHD and TD groups to serve as the classification features. We exploit several classifiers (ANN, SVM, KNN, and LDA) to discriminate between ADHD and TD groups. The Combination of dDTF measures at all frequency bands had very good accuracy (98%). The best result (99%) was achieved by the fusion of linear and nonlinear connectivity values of nCREANN methods. Up to our knowledge, this is one of the best classification accuracy among the studies that tried to discriminate between ADHD and TD subjects. Using the same dataset as ours, Ekhlasi et al., achieved the highest accuracy based on directed Phase Transfer Entropy (dPTE) measures at the theta frequency band with 89.7% [14]. Applying a convolutional, deep learning algorithm based on the mutual information (MI) to quantify the synchronization between EEG channels, Chen et al., reported accuracy of 94.67% %for detecting ADHDs from TD subjects [43]. In an effective connectivity study, Muthuraman et al., used all measures from the five different frequency bands of EEGs and attained 98% accuracy [44].

5. Conclusion

The linear and nonlinear effective connectivity measures of nCREANN method for ADHD subjects revealed various abnormalities in their connectivity patterns in comparison with TD individuals. The ADHD group showed reduced linear connectivity from temporal to frontal and occipital regions, the significant asymmetry between the two hemispheres with more interactions in the left hemisphere, and a thorough decrement in nonlinear connectivity compared to the TD group. Based on these effective connectivity measures we achieved the excellent classification accuracy in comparison with previous studies. For more generalization of reliable detection of ADHD subjects, applying the methods of this study on several big datasets would be considered as future works. Furthermore, applying the nCREANN on a dataset including both resting state and some mental task would help to achieve new insight into the nonlinear interaction patterns of the brain in healthy and ADHD subjects.

None declared

This study was supported by the Deputy of Research and Technology of Shahed University.

Acknowledgement

This study was supported by the Deputy of Research and Technology of Shahed University.

References

[1] A. Konrad, T.F. Dielentheis, D. El Masri, M. Bayerl, C. Fehr, T. Gesierich, G. Winterer, Disturbed structural connectivity is related to inattention and impulsivity in adult attention deficit hyperactivity disorder, Eur. J. Neurosci. 31 (5) (2010) 912–919.
[2] R.B. Silberstein, A. Pipingas, M. Farrow, F. Levy, C.K. Stough, D.A. Camfield, Brain functional connectivity abnormalities in attention-deficit hyperactivity disorder, Brain Behav. 6 (12) (2016), e00583, https://doi.org/10.1002/brb3.583.
[3] G. Deco, M.L. Kringelbach, Metastability and coherence: extending the communication through coherence hypothesis using A whole-brain computational perspective, Trends Neurosci. 39 (3) (2016) 125–135, https://doi.org/10.1016/j.tins.2016.01.001.
[4] I. Mohammad-Rezazadeh, J. Frohlich, S.K. Loo, S.S. Jeste, Brain connectivity in autism spectrum disorder, Curr. Opin. Neurol. 29 (2) (2016) 137–147, https://doi.org/10.1097/WCO.0000000000000301.
[5] A. Cubillo, R. Halari, C. Ecker, V. Giampietro, E. Taylor, K. Rubia, Reduced activation and inter-regional functional connectivity of fronto-striatal networks in adults with childhood Attention-Deficit Hyperactivity Disorder (ADHD) and persisting symptoms during tasks of motor inhibition and cognitive switching, J. Psychiatr. Res. 44 (10) (2010) 629–639.
[6] J. Posner, B.J. Nagel, T.V. Maia, A. Mechling, M. Oh, Z. Wang, B.S. Peterson, Abnormal amygdalar activation and connectivity in adolescents with attention-deficit/hyperactivity disorder, J. Am. Acad. Child Adolesc. Psychiatr. 50 (8) (2011) 828–837, https://doi.org/10.1016/j.jaac.2011.05.010, e823.
[7] C. Chen, H. Yang, Y. Du, G. Zhai, H. Xiong, D. Yao, F. Li, Altered functional connectivity in children with ADHD revealed by scalp EEG: an ERP study, Neural Plast. 2021 (2021), 6615384, https://doi.org/10.1155/2021/6615384.
[8] R. Debnath, N.V. Miller, S. Morales, K.R. Seddio, N.A. Fox, Investigating brain electrical activity and functional connectivity in adolescents with clinically elevated levels of ADHD symptoms in alpha frequency band, Brain Res. 1750 (2021), 147142, https://doi.org/10.1016/j.brainres.2020.147142.

[9] M. Murias, J.M. Swanson, R. Srinivasan, Functional connectivity of frontal cortex in healthy and ADHD children reflected in EEG coherence, Cerebr. Cortex 17 (8) (2006) 1788–1799, https://doi.org/10.1093/cercor/bhl089.
[10] S. Ansari Nasab, S. Panahi, F. Ghassemi, S. Jafari, K. Rajagopal, D. Ghosh, M. Perc, Functional neuronal networks reveal emotional processing differences in children with ADHD, Cognit. Neurodynam. (2021), https://doi.org/10.1007/s11571-021-09699-6.
[11] J.J. González, L.D. Méndez, S. Mañas, M.R. Duque, E. Pereda, L. De Vera, Performance analysis of univariate and multivariate EEG measurements in the diagnosis of ADHD, Clin. Neurophysiol. 124 (6) (2013) 1139–1150.
[12] K.J. Friston, Functional and effective connectivity in neuroimaging: a synthesis, Hum. Brain Mapp. 2 (1-2) (1994) 56–78, https://doi.org/10.1002/hbm.460020107.
[13] N. Talebi, A.M. Nasrabadi, I. Mohammad-Rezazadeh, R. Coben, nCREANN: nonlinear causal relationship estimation by artificial neural network; applied for autism connectivity study, IEEE Trans. Med. Imag. 38 (12) (2019) 2883–2890, https://doi.org/10.1109/TMI.2019.2916233.
[14] A. Ekhlasi, A. Motie Nasrabadi, M. Mohammadi, Classification of the children with ADHD and healthy children based on the directed phase transfer entropy of EEG signals, Front. Biomed. Technol. 8 (2) (2021), https://doi.org/10.18502/fbt.v8i2.6515.
[15] A. Ekhlasi, A.M. Nasrabadi, M.R. Mohammadi, Direction of information flow between brain regions in ADHD and healthy children based on EEG by using directed phase transfer entropy, Cognit. Neurodynam. (2021), https://doi.org/10.1007/s11571-021-09680-3.
[16] A.K. Abbas, G. Azemi, S. Amiri, S. Ravanshadi, A. Omidvarnia, Effective connectivity in brain networks estimated using EEG signals is altered in children with ADHD, Comput. Biol. Med. 134 (2021), 104515, https://doi.org/10.1016/j.compbiomed.2021.104515.
[17] A. Motie Nasrabadi, A. Allahverdy, M. Samavati, M.R. Mohammadi, EEG Data for ADHD/Control Children, 2020.
[18] D. American Psychiatric Association, A.P. Association, Diagnostic and Statistical Manual of Mental Disorders: DSM-5, vol. 5, American psychiatric association Washington, DC, 2013.
[19] A. Armin, M. Alireza Khorrami, M. Mohammad Reza, N. Ali Motie, Detecting ADHD children using the attention continuity as nonlinear feature of EEG, Front. Biomed. Technol. 3 (1–2) (2016).
[20] A. Delorme, S. Makeig, EEGLAB: an open source toolbox for analysis of single-trial EEG dynamics including independent component analysis, J. Neurosci. Methods 134 (1) (2004) 9–21, https://doi.org/10.1016/j.jneumeth.2003.10.009.
[21] X. Jiang, G.-B. Bian, Z. Tian, Removal of artifacts from EEG signals: a review, Sensors 19 (5) (2019) 987, https://doi.org/10.3390/s19050987.
[22] M.M.N. Mannan, M.A. Kamran, M.Y. Jeong, Identification and removal of physiological artifacts from electroencephalogram signals: a review, IEEE Access 6 (2018) 30630–30652, https://doi.org/10.1109/ACCESS.2018.2842082.
[23] J.A. Urigüen, B. Garcia-Zapirain, EEG artifact removal—state-of-the-art and guidelines, J. Neural. Eng. 12 (3) (2015), 031001, https://doi.org/10.1088/1741-2560/12/3/031001.
[24] P.L. Nunez, R. Srinivasan, Electric Fields of the Brain: the Neurophysics of EEG, Oxford university press, 2006.
[25] K. Friston, L. Harrison, J. Daunizeau, S. Kiebel, C. Phillips, N. Trujillo-Barreto, J. Mattout, Multiple sparse priors for the M/EEG inverse problem, Neuroimage 39 (3) (2008) 1104–1120, https://doi.org/10.1016/j.neuroimage.2007.09.048.
[26] A. Korzeniewska, M. Mańczak, M. Kamiński, K.J. Blinowska, S. Kasicki, Determination of information flow direction among brain structures by a modified directed transfer function (dDTF) method, J. Neurosci. Methods 125 (1) (2003) 195–207, https://doi.org/10.1016/S0165-0270(03)00052-9.
[27] A. Delorme, T. Mullen, C. Kothe, Z. Akalin Acar, N. Bigdely-Shamlo, A. Vankov, S. Makeig, EEGLAB, SIFT, NFT, BCILAB, and ERICA: new tools for advanced EEG processing, Comput. Intell. Neurosci. 2011 (2011), 130714, https://doi.org/10.1155/2011/130714.
[28] T. Schneider, A. Neumaier, Algorithm 808: ARfit—a Matlab package for the estimation of parameters and eigenmodes of multivariate autoregressive models, ACM Trans. Math Software 27 (1) (2001) 58–65.
[29] K. Benmouiza, A. Cheknane, Forecasting hourly global solar radiation using hybrid k-means and nonlinear autoregressive neural network models, Energy Convers. Manag. 75 (2013) 561–569, https://doi.org/10.1016/j.enconman.2013.07.003.
[30] N. Talebi, A.M. Nasrabadi, I. Mohammad-Rezazadeh, Estimation of effective connectivity using multi-layer perceptron artificial neural network, Cognit. Neurodynam. 12 (1) (2018) 21–42, https://doi.org/10.1007/s11571-017-9453-1.
[31] C.M. Jarque, A.K. Bera, Efficient tests for normality, homoscedasticity and serial independence of regression residuals, Econ. Lett. 6 (3) (1980) 255–259, https://doi.org/10.1016/0165-1765(80)90024-5.
[32] R.F. Woolson, Wilcoxon Signed-Rank Test *Wiley Encyclopedia Of Clinical Trials*, 2008, pp. 1–3.
[33] J.N. Epstein, M.P. DelBello, C.M. Adler, M. Altaye, M. Kramer, N.P. Mills, S. Holland, Differential patterns of brain activation over time in adolescents with and without attention deficit hyperactivity disorder (ADHD) during performance of a sustained attention task, Neuropediatrics 40 (2009) 1–5, 01.
[34] M. Cao, J.M. Halperin, X. Li, Abnormal functional network topology and its dynamics during sustained attention processing significantly implicate post-TBI attention deficits in children, Brain Sci. 11 (10) (2021) 1348.
[35] S. Xia, J. Foxe, A. Sroubek, C. Branch, X. Li, Topological organization of the "small-world" visual attention network in children with attention deficit/hyperactivity disorder (ADHD), Front. Hum. Neurosci. 8 (2014), https://doi.org/10.3389/fnhum.2014.00162.
[36] K. Rubia, A. Cubillo, A.B. Smith, J. Woolley, I. Heyman, M.J. Brammer, Disorder-specific dysfunction in right inferior prefrontal cortex during two inhibition tasks in boys with attention-deficit hyperactivity disorder compared to boys with obsessive–compulsive disorder, Hum. Brain Mapp. 31 (2) (2010) 287–299, https://doi.org/10.1002/hbm.20864.
[37] C.-T. Chiang, C.-S. Ouyang, R.-C. Yang, R.-C. Wu, L.-C. Lin, Increased temporal lobe beta activity in boys with attention-deficit hyperactivity disorder by LORETA analysis, Front. Behav. Neurosci. 14 (85) (2020), https://doi.org/10.3389/fnbeh.2020.00085.
[38] F.E. Dupuy, A.R. Clarke, R.J. Barry, R. McCarthy, M. Selikowitz, EEG coherence in girls with Attention-Deficit/Hyperactivity Disorder: stimulant effects in good responders, Int. J. Psychophysiol. 70 (3) (2008) 151–157, https://doi.org/10.1016/j.ijpsycho.2008.07.012.
[39] N. Makris, J. Biederman, E.M. Valera, G. Bush, J. Kaiser, D.N. Kennedy, L. J. Seidman, Cortical thinning of the attention and executive function networks in adults with attention-deficit/hyperactivity disorder, Cerebr. Cortex 17 (6) (2006) 1364–1375, https://doi.org/10.1093/cercor/bhl047.
[40] H.M. Geurts, K.R. Ridderinkhof, H.S. Scholte, The relationship between grey-matter and ASD and ADHD traits in typical adults, J. Autism Dev. Disord. 43 (7) (2013) 1630–1641, https://doi.org/10.1007/s10803-012-1708-4.
[41] H. Sohn, I. Kim, W. Lee, B.S. Peterson, H. Hong, J.-H. Chae, J. Jeong, Linear and non-linear EEG analysis of adolescents with attention-deficit/hyperactivity disorder during a cognitive task, Clin. Neurophysiol. 121 (11) (2010) 1863–1870, https://doi.org/10.1016/j.clinph.2010.04.007.
[42] A. Fernández, J. Quintero, R. Hornero, P. Zuluaga, M. Navas, C. Gómez, T. Ortiz, Complexity analysis of spontaneous brain activity in attention-deficit/hyperactivity disorder: diagnostic implications, Biol. Psychiatr. 65 (7) (2009) 571–577, https://doi.org/10.1016/j.biopsych.2008.10.046.
[43] H. Chen, Y. Song, X. Li, A deep learning framework for identifying children with ADHD using an EEG-based brain network, Neurocomputing 356 (2019) 83–96, https://doi.org/10.1016/j.neucom.2019.04.058.
[44] Muthuraman Muthuraman, Vera Moliadze, Lena Boecher, Julia Siemann, Christine M. Freitag, Sergiu Groppa, Michael Siniatchkin, Multimodal alterations of directed connectivity profiles in patients with attention-deficit/hyperactivity disorders, Sci. Rep. 9 (1) (2019), https://doi.org/10.1038/s41598-019-56398-8.
[45] Fabio Babiloni, Febo Cincotti, Claudio Babiloni, Filippo Carducci, Donatella Mattia, Laura Astolfi, Alessandra Basilisco, Paolo Maria Rossini, Lei Ding, Yicheng Ni, Estimation of the cortical functional connectivity with the multimodal integration of high-resolution EEG and fMRI data by directed transfer function, Neuroimage 24 (1) (2005) 118–131.
[46] Cornelis J Stam, Nonlinear dynamical analysis of EEG and MEG: review of an emerging field, Clin. Neurophysiol. 116 (10) (2005).
[47] Huanfei Ma, Kazuyuki Aihara, Luonan Chen, Detecting causality from nonlinear dynamics with short-term time series, Sci. Rep. 4 (2014).